Structural Engineering and Mechanics, Vol. 36, No. 6 (2010) 745-758
DOI: http://dx.doi.org/10.12989/sem.2010.36.6.745

Cyclic load experiment study on the laminated composite RC walls with different concrete ages

Hongmei Zhang*, Xilin Lu[a], Jianbao Li[b] and Lin Liang[c]

State Key Laboratory of Disaster Reduction in Civil Engineering, Tongji University, Shanghai, China

(Received October 1, 2009, Accepted September 1, 2010)

Abstract. 12 typical laminated composite reinforced concrete (RC) walls with different concrete ages and 3 cast-in-place RC walls subjected to low frequency cyclic load were carried out in this study. The failure mode, force-deformation response and energy dissipation capacity of these specimens were investigated. Differences of structural behaviours between composite RC walls and common cast-in-place RC walls were emphasized in the analysis. The compatibility of the composite specimens with different concrete ages was discussed based on the experiment. Test results indicated that the differences between the lateral bearing capacity and the displacement ductility of the composite walls and the common walls were not so obvious. Some of the composite specimen even has higher bearing capacity under the experiment loading situation. Besides, the two parts of the laminated composite specimens demonstrates incompatibility at the later loading sequence on failure mode and strain response when it is in tension. Finally, this laminated composite shear walls are suggested to be applied in rapid reconstruction structures which is not very high.

Keywords: different concrete ages; prefabricated wall; cast-in-place; laminated composite wall; cyclic loading test; compatibility.

1. Introduction

Reinforced concrete (RC) shear wall is a kind of earthquake resistant structure member which can provide large potential of lateral and axial bearing capacity, and it is widely used in high rise buildings. To day, research and innovation on the construction and improving on RC walls is a main task for researchers and engineers.

Prefabricate reinforced concrete (PRC) shear walls have already been used in Japan, Germany and Europe (Saito *et al*. 1995, Holden *et al*. 2003, Schmitz *et al*. 2006, Mark 2001). Prefabricated sandwich panels (Gong *et al*. 2004, Kabir *et al*. 2007) and multi-bay coupled shear walls (Bozdogan *et al*. 2008) has been investigated by experiments. To day, a new type of half prefabricated half cast-in-place laminated composite RC shear wall has been applied in China. This kind of prefabricate RC shear wall contains both horizontal and vertical steel bars (Makoto *et al*. 1995), and

*Corresponding author, Lecturer, E-mail: zhanghongmei@tongji.edu.cn
[a]Professor
[b]Lecturer
[c]Ph.D. Student

the embedded columns could also be set like common RC walls. This kind of laminated composite wall can be partly manufactured in factory, and the windows and surface decoration can be prefabricated also. Therefore, the site work can be greatly reduced, and the installation quality can be efficiently confirmed.

The constitution method of the composite wall is similar to common cast-in-place walls, but the bearing capacity, the deformation response and other structural behaviour still have not been verified by relative experiments. In order to investigate the structural behaviour of this laminated composite wall with different concrete ages, composite RC wall specimens subjected to low frequency cyclic loads were studied in this paper. Through a series of reversed cyclic loading tests, the failure mode, the deformation ductility and the energy dissipation capacity of these specimens were investigated and analyzed. The study could provide reference to the shear wall design on rapid reconstruction.

2. Experimental Investigation

2.1 Specimen Introduction

The bonding capacity and the compatibility will influence the structural behaviour of the composite walls, but to the details, it still remains vague. To clarify the uncertainty, 15 composite RC walls subjected to low frequency cyclic loads were studied. These specimens include: (a) half solid prefabricated composite shear walls (PCFA) and the conventional cast-in-place wall (SWA);

Table 1 Details of the specimen section

Specimen name	Embedded column parameters			Distributing bars (HRB400)	Axial force (kN)	Specimen description
	Dimension (mm)	Longitudinal bars (HRB335)	Stirrup bars (HRB400)	Longitudinal / vertical		
PCFA1 PCFA2 PCFA3 PCFA4	180×400	6⌀14	⌀8@150	⌀8@150	1200	Composite wall
PCFB1 PCFB2 PCFB3 PCFB4	180×400	6⌀14	⌀8@150	⌀8@150	600	Composite wall
PCFC1 PCFC2 PCFC3 PCFC4	180×400	6⌀14	⌀8@150	⌀8@150	1200	Composite wall
SWA	250×400	6⌀14	⌀8@150	⌀8@150	1200	Common cast-in-place wall
SWB	250×400	6⌀14	⌀8@150	⌀8@150	600	Common cast-in-place wall
SWC	250×400	6⌀14	⌀8@150	⌀8@150	1200	Common cast-in-place wall

Note: dimension of the specimens: 1800 mm×1500 mm×250 mm.

(b) half prefabricate composite shear walls with an opening in centre (PCFB) and the conventional cast-in-place wall (SWB); (c) half prefabricate composite shear walls with a vertical slit (PCFC) and the conventional cast-in-place wall (SWC). Each specimen is 1500 mm in length, 1800 mm in height and 250 mm in thickness. Strengthening bars were put at the top and bottom of the specimens to enhance the connection of the prefabricated part to the top and bottom beam, which was set as HRB40Φ 10@150 (HRB means the high strength steel, and the yield strength of the steel mentioned here is 400 MPa). Embedded columns were located at the edge of the wall, and the longitudinal bars were set in the cast-in-place part. The embedded columns and the longitudinal reinforcement were designed abide by the design code for design of concrete structures of China (GB50020-2002) (Gong *et al*. 2006, Zhang *et al*. 2007). The dimensions, reinforcement sizes and axial load capacity of the tested specimens are listed in Table 1.

Horizontal and vertical trusses were set across the prefabricated and the cast-in-place parts to enhance the interfacial bonding capacity of the composite specimens. A layout of internal trusses is shown in Fig. 1(a). Horizontal and vertical distribution bars were also set in the prefabricated part like common shear walls. The steel truss is composed of the upper and lower truss bars, which are connected by web bars. The lower truss bar is bounded into the steel cage of the prefabricated part when the prefabricated part is made in factory. The distribution diagram of the truss bars and the

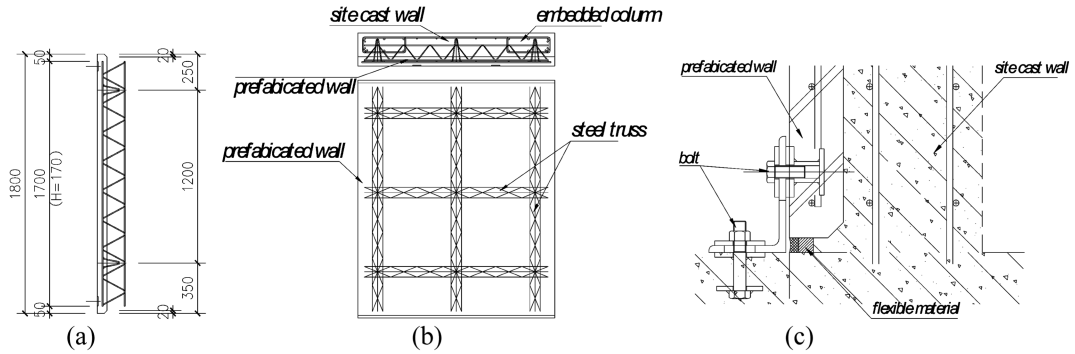

Fig. 1 Construction diagram of steel truss (a) section of prefabricated part, (b) diagram of connection truss, (c) assemble method of the laminated wall

Fig. 2 Manufacturing process of the specimens (a) prefabricated walls, (b) binding process of the steel bars in cast-in-place part

fabricated part are shown in Fig. 1(b). The steel trusses crossing the prefabricated part and the cast-in-place part could efficiently promote the connection strength. The local connection of the composite wall is shown in Fig. 1(c). The prefabricated part was fixed to the basement by bolts when it is just erected, and the cast-in-place part was cast in the traditional way.

The manufacture process of the composite wall specimens is shown in Fig. 2. The bond steel truss sticking out of the prefabricated concrete part is demonstrated in Fig. 2(a). And Fig. 2(b) shows the binding process of the steel bars in the cast-in-place part.

2.2 Material property

When the cast-in-place walls parts were constructed, concrete material test cubes were made simultaneously. The test concrete blocks contains two kinds of dimensions, one is 100 mm × 100 mm × 300 mm and the other is 150 mm × 150 mm × 150 mm. The main steel bars used in the specimens were also tested. Material property result can be found in Table 2 and Table 3.

2.3 Experiment program

The testing rig and the loading sequence are shown in Fig. 3. Specimen was fixed in the steel frame, and the horizontal load was applied by electro-hydraulic servo loading device. Vertical axial pressure was applied by jacks on the top beam of the wall. Each jack can provide 30 kN vertical load, and there were 4 jacks seated on the loading beam of the solid specimens and 2 jacks on the specimens with an opening. The vertical load was designed according to the typical loading

Table 2 Concrete material property

Specimen number	f_{cu} / MPa	f_c / MPa	E_c / N m^{-2}
PCFII-A	27.7	23.8	3.35×10^{10}
PCFII-B	33.6	27.8	3.66×10^{10}
PCFII-C	35.3	31.0	3.14×10^{10}
SWA	27.7	19.7	2.90×10^{10}
SWB	32.4	28.7	3.06×10^{10}
SWC	30.0	19.5	2.98×10^{10}

f_{cu}: concrete cube compression strength, f_c: concrete axis compression strength, E_c: concrete elastic modulus.

Table 3 Steel material properties

Steel bar type	Diameter	f_y / MPa	f_u / MPa	E_s / N m^{-2}	ε_y / $\mu\varepsilon$
ϕ14	14 mm	372.80	546.93	2.0×10^{11}	1864
ϕ12	12 mm	371.67	535.2	2.01×10^{11}	1849
⌽10	10 mm	380.24	604.5	2.0×10^{11}	1901
⌽8	8 mm	385.03	617.04	2.0×10^{11}	1925

f_y: tested yield tension strength, f_u: tested ultimate tension strength, E_s: steel bar elastic modulus, ε_y: yield strain

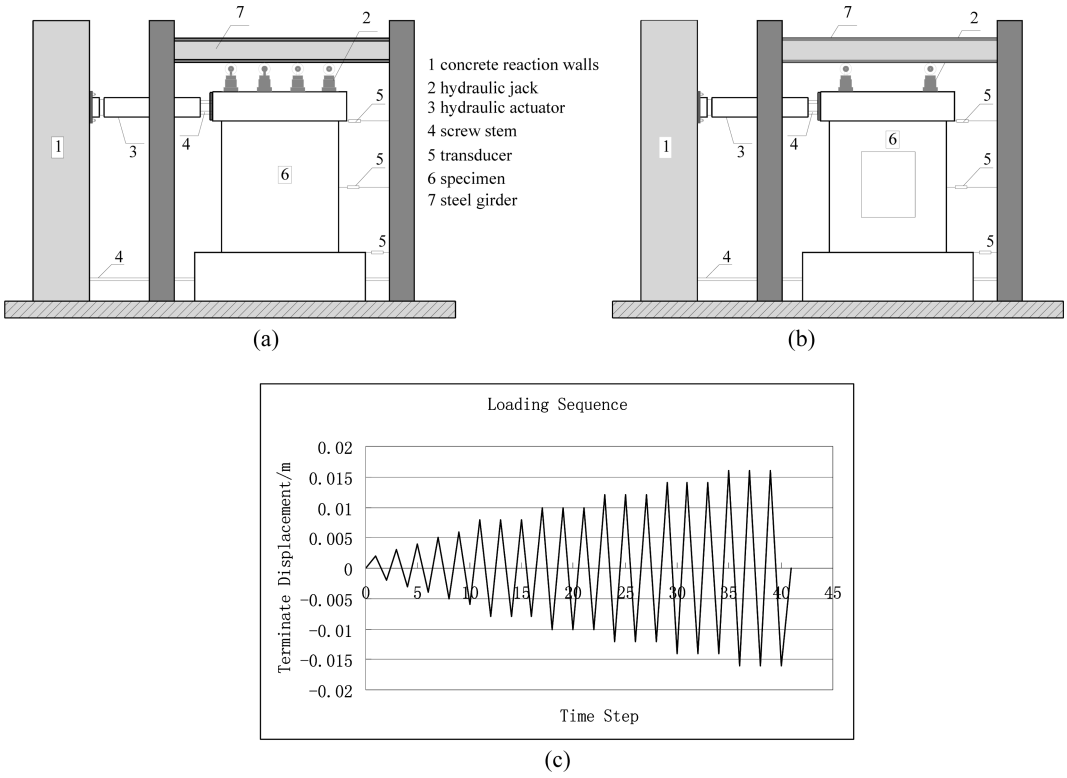

Fig. 3 Testing rig and loading sequence (a) Test rig of solid specimen, (b) Test rig of specimen with an opening, (c) Loading sequence

situation of the shear walls. The test rig and loading sequence are shown in Fig. 3. Fig. 3(a) demonstrates the test rig of solid walls, Fig. 3(b) shows that of walls with an opening, and Fig. 3(c) shows the typical loading sequence.

All the specimens were loaded by a constant vertical load and reversed cyclic lateral displacement. Horizontal load was applied by displacement-controlled loading method. The vertical load was imposed to 1200 kN (the design load) before the lateral load was applied, and it maintained to a constant pressure during the test (Salonikios *et al*. 1999).

During the lateral loading procedure, each displacement step was increased by 1 mm firstly, and every load sequence maintains for one cycle. After that, each step was increased by 2 mm when the specimen became yield and every load stage was kept for three cycles. The specimen was declared failed when the lateral force decreased to 85% of the maximum lateral bearing value.

3. Experiment results analyses

3.1 Failure mode

In general, specimens were maintained elastic until top displacement reached 4 to 8 mm at the early stage of the loading procedure. Short horizontal and inclined cracks appeared at the corner of

the cast-in-place part firstly, and then extend to the lower corner of the prefabricated part for the composite specimens. Cracks were closed during the unloading procedure at the early plastic stage of the specimens. The cracks kept growing in length and width during the loading procedure. And the rigidity decreased with the increase of the loading, while the decreasing ratio became smaller. Lateral force resistance degraded at the later stage of the load sequence and almost decreased to 85% of the maximum value when the displacement reached 30 mm to 46 mm. And then, concrete at the lower corner of the specimen crushed (see from Fig. 4 to Fig. 6), and the test came to the end.

The typical crack propagation process and failure mode of the three groups of composite specimens are shown in Fig. 4 to Fig. 6 respectively. The comparing results of the three types of composite walls indicate that the solid walls and the walls with a slit have higher lateral resisting

(a) Prefabricated part (b) Cast-in-place part

Fig. 4 Crack distribution and failure mode of the solid composite wall

(a) Prefabricated part (b) Cast-in-place part

Fig. 5 Crack distribution and failure mode of the composite wall with an opening

(a) Prefabricated part (b) Cast-in-place part

Fig. 6 Crack distribution and failure mode of the composite wall with a slit

capacity. The cracks concentrate at the lower part of the specimens, and they are not as plentiful as those of the specimen with an opening.

The test results give out the information that the damage mode of the prefabricated side and the cast-in-place side of the solid composite specimens behaved almost in the same pattern, which indicated that the deformation of the two parts concrete with different ages agree to each other in general. The same crack scattering and failure pattern were also observed on composite specimens with an opening. The concrete at the corner crushed when the composite specimens with a slit failed. And the damage seems more serious on the cast-in-place side. Moreover, the crack was observed not continuous at the two sides of the slit. Therefore obviously, the slit can dissipate part of the energy, and so as to reduce the damage.

3.2 Lateral force-displacement hysteretic relationship

The force-top displacement hysteretic curve could be drawn by the data collection system. Lateral force-top displacement hysteretic curve of the three groups of composite walls are shown in Fig. 7 to Fig. 9, and the curve of the conventional RC walls are displayed in Fig. 10. The skeleton curves of each group of specimens are shown in Fig. 11, including the conventional cast-in-place RC walls. The force-top displacement hysteretic curves demonstrate that the force-top displacement hysteretic curves of composite walls are quite similar to those of the conventional walls. The lateral bearing capacity and displacement ductility ratio of composite walls are no less than those of conventional RC walls.

The hysteretic hoops are shown in Fig. 7 to Fig. 10. Two features can be found by the comparison of Fig. 7 and Fig. 10. First of all, the hysteretic hoops of the solid composite walls are plumper than that of the conventional walls. Moreover, the initial rigidity of the composite walls is stronger than that of the conventional walls. The above two features could provide evidence to that the quality of the prefabricated parts can be efficiently confirmed in factory, and the initial rigidity is higher than the cast-in-place one. Besides, the damage may occur later than the cast-in-place part, so the plastic deformation have not emerged in the same time with the cast-in-place part, and the energy

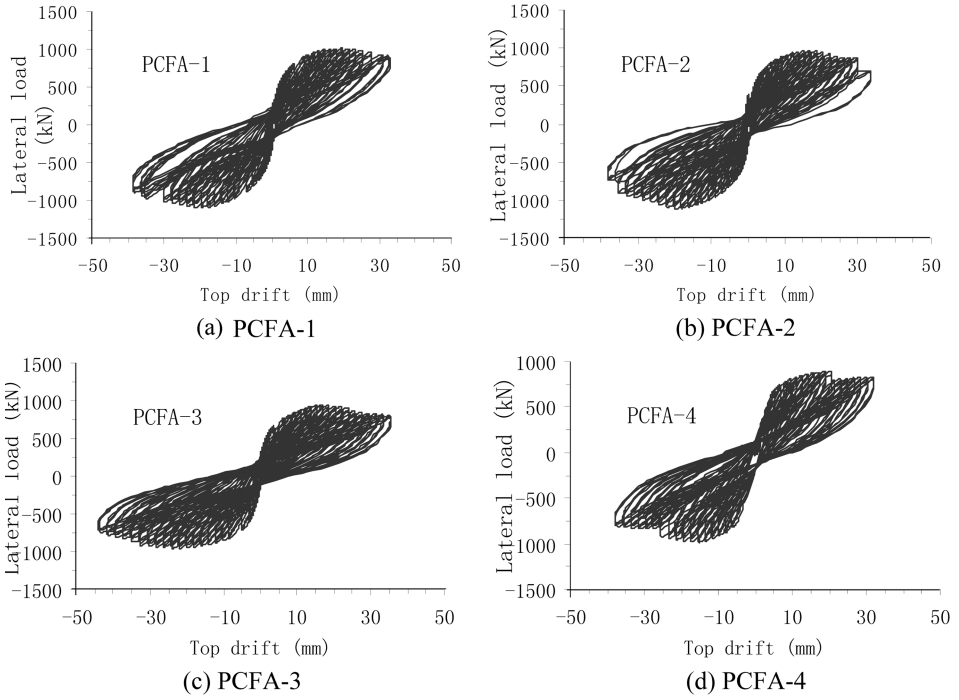

(a) PCFA-1 (b) PCFA-2

(c) PCFA-3 (d) PCFA-4

Fig. 7 Lateral load-top displacement curve of solid composite walls

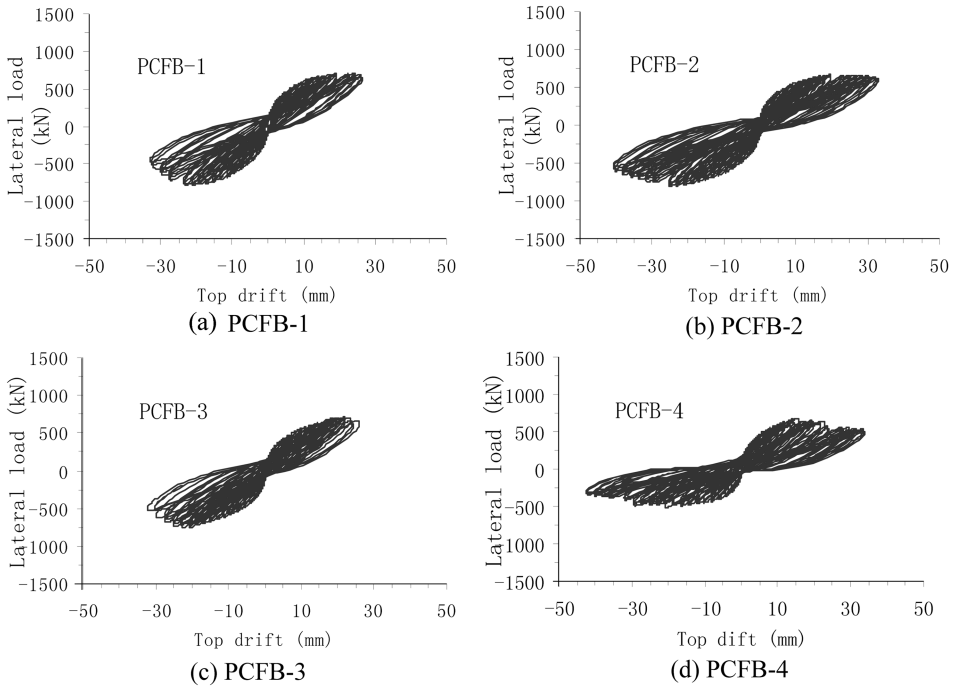

(a) PCFB-1 (b) PCFB-2

(c) PCFB-3 (d) PCFB-4

Fig. 8 Lateral load-top displacement curve of composite walls with an opening

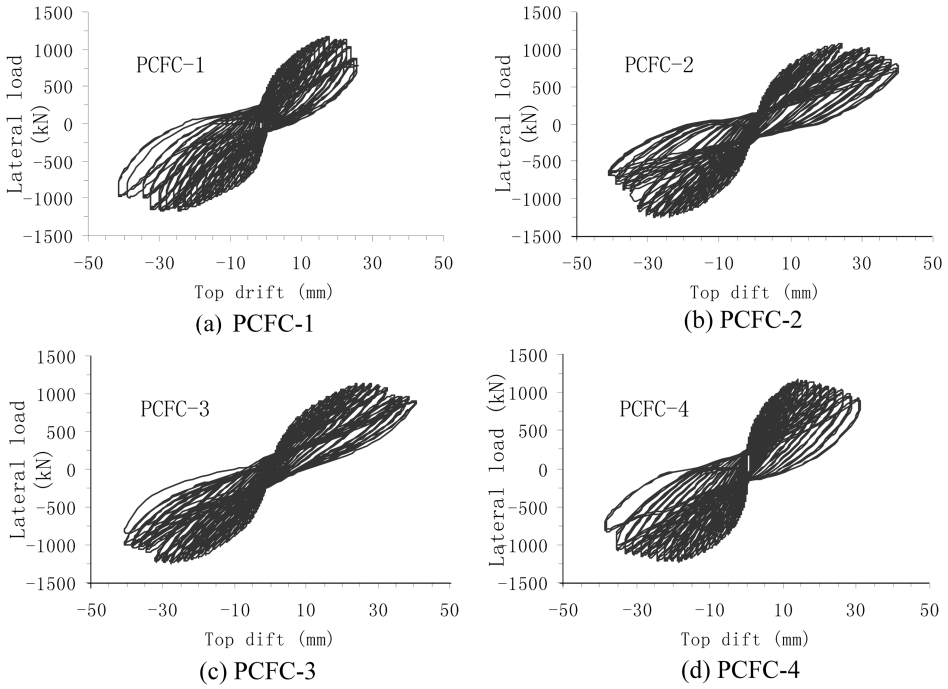

Fig. 9 Lateral load-top displacement curve of composite walls with a slit

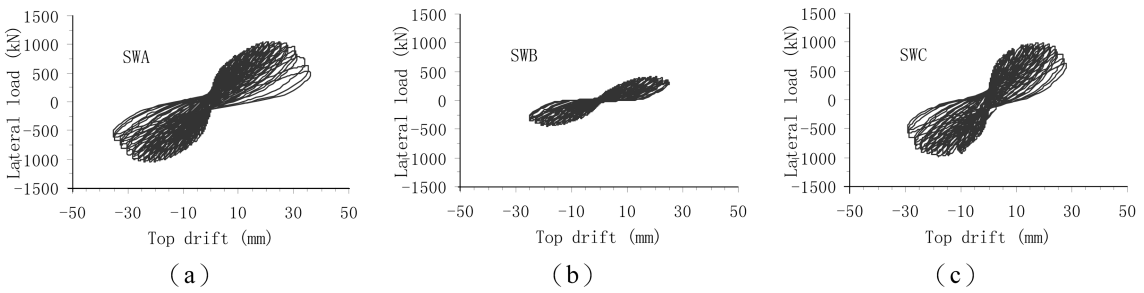

Fig. 10 Lateral load-top displacement curve of the cast-in-place conventional RC walls (a) Cast-in-place solid walls, (b) Cast-in-place walls with an opening, (c) Cast-in-place walls with a slit

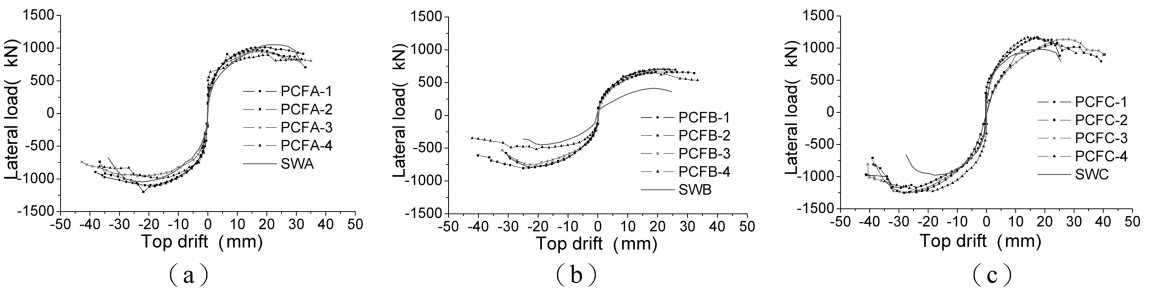

Fig. 11 Force-displacement skeleton curve (a) Solid specimens, (b) Specimens with an opening, (c) Specimens with a slit

dissipation effect of the prefabricated part has not totally take into action.

The initial stronger rigidity feature is also observed in group of PCFB and specimen SWB. But the lateral bearing capacity of the composite walls are higher than that of the conventional specimen SWB, which may attribute to the strengthening of the connection beam of the composite walls.

Hysteretic hoops of specimen group PCFC are plumper than that of SWC which can be observed in Fig. 9 and Fig. 10. The hysteretic hoops of the composite walls of this group are narrower than that of SWC. The delay of the plastic deformation may attribute to the narrow hoops. And the slit in the middle of the composite specimens could weaken the initial rigidity, so the initial rigidity difference is not so distinct than group PCFA.

3.3 Structural property results analysis

Some of the test results including the displacement ductility ratio are listed in Table 4 to 6. It could be observed from Table 4 to Table 6 that the lateral load resistant capacity and the lateral load-top drift curve of each group of the composite walls agree with each other, which could manifests the stability of the test results. The ductility ratios mentioned in Table 4 are defined as the ultimate displacement to the yield displacement, which is employed to evaluate the deformation capacity of the composite walls.

Table 4 Forcedisplacement property of the solid walls

Specimen number	Axial force (kN)	Axial ratio	Cracking load P_{cr} (kN)	Cracking displacement Δ_{cr} (mm)	Yield load P_y (kN)	Yield displacement Δ_y (mm)	Maximum load P_m (kN)	Ultimate load P_u (kN)	Ultimate displacement Δ_u (mm)	Displacement ductility μ
PCFIIA1	1200	0.11	760	5.02	900	9.0	1012	860	32.4	3.60
PCFIIA2	1200	0.11	756	5.16	886	9.3	1045	888	30.0	3.22
PCFIIA3	1200	0.11	727	5.12	846	9.5	950	807	33.0	3.47
PCFIIA4	1200	0.11	693	5.32	803	9.6	915	778	31.0	3.23
SWA	1200	0.11	600	4.04	738	7.5	1053	895	26.0	3.45

*Note: Cracking load, First yield and Ultimate load all mean the lateral load. The yield point defined as the cross point related to the secant line of the 75% peak strength. The ultimate point is defined as the point when the lateral force decreased to 85% of the peak lateral force value or the specimen failure point on the forcedisplacement curve.

Table 5 Forcedisplacement property of the walls with an opening

Specimen number	Axial force (kN)	Axial ratio	Cracking load P_{cr} (kN)	Cracking displacement Δ_{cr} (mm)	Yield load P_y (kN)	Yield displacement Δ_y (mm)	Maximum load P_m (kN)	Ultimate load P_u (kN)	Ultimate displacement Δ_u (mm)	Displacement ductility μ
PCFIIB1	600	0.11	459.35	5.02	623.39	10.90	793	589.93	29.9	2.74
PCFIIB2	600	0.11	486.50	6.99	581.09	11.37	805	611.01	40.1	3.52
PCFIIB3	600	0.11	477.42	6.74	586.24	11.37	755	532.33	32.0	2.81
PCFIIB4	600	0.11	508.42	6.45	627.46	11.76	677	543.71	31.0	2.63
SWB	600	0.11	201.50	3.00	260.80	4.92	446	379.00	18.8	3.82

Table 6 Forcedisplacement properties of the walls with a slit

Specimen number	Axial force (kN)	Cracking load P_{cr} (kN)	Cracking displacement Δ_{cr} (mm)	Yield load P_y (kN)	Yield displacement Δ_y (mm)	Maximum load P_m (kN)	Ultimate load P_u (kN)	Ultimate displacement Δ_u (mm)	Displacement ductility μ
PCFIIC1	1200	785	6.84	930	12.11	1174	998	41.5	3.43
PCFIIC2	1200	912	5.96	963	12.15	1251	1064	41.0	3.38
PCFIIC3	1200	890	5.81	850	12.21	950	968	40.3	3.30
PCFIIC4	1200	932	6.69	993	10.68	1225	1041	38.6	3.62
SWC	1200	638	3.84	718	4.33	980	833	19.6	4.52

Table 4 demonstrates that the crack and the yield top displacement are 27.6% and 24.7% larger than that of the conventional RC walls. That also indicates that the qualified fabricated part can delay the cracking of the specimens. Besides, the lateral resist capacity and the displacement ductility are as well as the conventional RC walls.

From Table 5 it could be found that the lateral resist capacity or the yield displacement of the composite specimens with an opening is larger by 100% and 130% than the conventional RC walls. That may attribute to the local strengthening method of the connection beam and the local area around the opening as above stated.

Lateral resist property of the composite specimens with a slit are shown in Table 6. The cracking load, the yield load and the ultimate load are all higher than that of the traditional RC walls. Further more, the initial crack, the yield and the ultimate displacement are also obviously larger than that of the traditional RC walls. This difference may be illustrated by the slit effect. The slit could allow larger lateral deformation and so as the energy could be dissipated more efficiently, and this slit effect is also demonstrated in relative paper (Lu *et al*. 2000).

3.4 Deformation compatibility of concrete with different ages

As the investigation concerned, the compatibility capacity of the two parts concrete with different ages of the half fabricated half cast-in-place composite wall is discussed here. That can be evaluated from the behavior of the interface cracking and the loading-deformation history in general.

The behavior of the three groups of specimens is similar to the regular RC walls under vertical pressure and lateral load. Tiny horizontal and inclined cracks emerged at the early stage of the loading sequence. And plenty of visible horizontal and inclined cracks could be found at the surface of the specimen when the lateral force nearly reached its ultimate value. Vertical cracks also could be found on the interface of the fabricated part and the cast-in-place part. Further more, the vertical crack developed with the increasing of the lateral displacement until the specimen was declared failed, and that is demonstrated in Fig. 12. Horizontal cracks at the edge were also found crossing the two concrete parts with different ages when the vertical crack emerged.

The steel bars alternated by tension and pressure during the cyclic loading procedure, and the damage accumulated gradually during the process. Strain gages were laid on the surface of the steel bars in the boundary area of the specimens. The vertical strain variation history of the longitudinal bars can be collected by the test equipment. The loading-strain variation history of the test is drawn in Fig. 13.

(a) Solid composite wall (b) Composite walls with an opening (c) Composite walls with a slit

Fig. 12 Crack distribution at the edge of the specimens

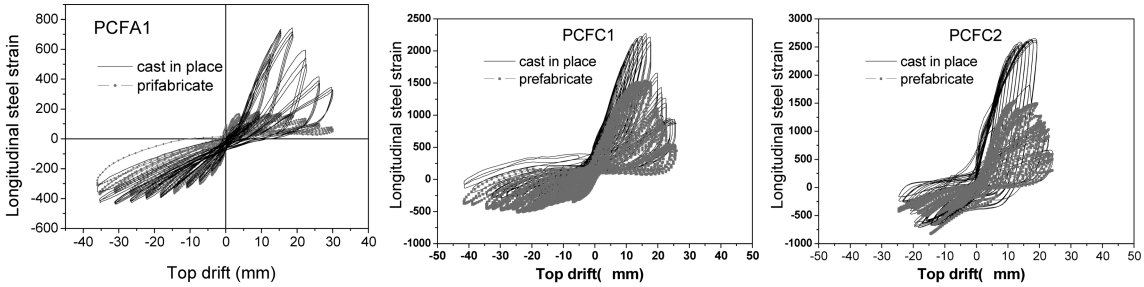

(a) Longitudinal steel strain of PCFA1 (b) Longitudinal steel strain of PCFC1 (c) Longitudinal steel strain of PCFC2

Fig. 13 Longitudinal steel strain development history comparison of the two parts of the specimens

The longitudinal steel strain development history is drawn in Fig. 13. This figure demonstrates the effective strain hoops of boundary steel bars collected from the test. Most of the strain data collected by the gages can not provide enough length of the loading history curve because of early damage of the gages.

The specimens were loaded by cyclical load during the loading procedure. And the loading and unloading procedure of tension and pressing are acted on the specimen alternately. The longitudinal steel bars was also enduring the process of tension and pressing. When the specimen was in pressing, both the edge concrete and the longitudinal bar were in pressing, and the longitudinal bar will work normally until the strain reached its measuring range, that may be about the strain value of 3000.

If the edge of the specimen was in tension, the concrete in the tension area can easily reach its crack strain limitation. And the strain value will develop fast if the strain gage is at the crack area. As to other situation, if the gage locates at the no crack area, the strain will develop on a small scale for the main deformation will concentrate at the crack area.

Fig. 13 demonstrates the strain development history of longitudinal steel bar at the prefabricated part and the cast-in-place part. The difference of the strain development could be found from the curve in the figure, which can provide a quantized incompatible value. From Fig. 13, it could be

deduced that the cast-in-place steel strain located near the crack for it developed fast at a certain value. And the tension strain of the steel strain at prefabricated part is within a low value since it located in the no crack area. The strain of the no crack area was small, for the deformation was mainly caused by the cracking. The compression strain of the prefabricated and the cast-in-place part in Fig. 13 are almost in same step, which may indicate the compatibility of the two concrete parts with different ages.

The situation of PCFC1 and PCFC2 seems similar to each other. When the boundary longitudinal steel is in tension, the steel strain in cast-in-place part is more sensitive and the amplitude value of the strain varies larger than that of the prefabricated part. It could give evidence to that the prefabricated part has better integrity, and the prefabricated part is delayed in vertical deformation. When the specimen edge is in compression, the difference of the strain value is not so obviously. As we know, the concrete compression capacity and deformation resist capacity could be enhanced as the confine effect. Therefore, when the edge of the specimen is in compression, the confine effect of the boundary concrete in cast-in-place area will play the role, which may illustrate the reason that the edge strain difference is not so distinct.

The test and the analysis results could provide the evidence that the prefabricated part and the cast-in-place part of the laminated composite walls are compatible when it is in compress. And the incompatible deformation may appear when the area is in tension. The vertical crack emerged at the interface of the concrete with different ages when the specimen was near to the maximum bearing value and the horizontal cracks appeared almost simultaneously. Concrete became crashed at the corner of the composite wall and developed to the end of the test. The incompatibility of the prefabricated part and the cast-in-place part demonstrated not so distinct even at the degradation stage of the nonlinear deformation developing procedure.

5. Conclusions

The structural property of the composite walls with different concrete ages is investigated in this paper. 15 RC shear walls were tested under reversed cyclic loads including 4 solid composite walls, 4 composite walls with an opening and 4 composite walls with a slit. And they are compared with 3 conventional RC walls. From the test and analysis results, the following conclusions could be drawn:

(a) The failure mode of the composite shear wall with different concrete ages is almost the same as the conventional walls. The prefabricated part has better integrity and failure is delayed.

(b) The force-displacement curve of the composite walls and the conventional walls are similar with each other. The bearing capacity and the initial rigidity are higher than that of the conventional one.

(c) The slit of the composite walls helps to dissipate the energy during the loading procedure.

(d) The prefabricated part and the cast-in-place part could work in step when it is in compression, and when it is in tension, the incompatibility still could not cause distinct inharmonious. The integrity of this kind of composite walls is not so different from a conventional one.

This investigation of the laminated composite wall may provide some reference to the composite wall design. The construction method may influence the compatibility of the wall and the edge concrete could be confined to have better integrity. And this kind of laminated composite wall is

expected to be applied in the building of common height and the joint of the wall to wall, wall to column, wall to beam should be treat as vulnerable parts to strength. Steel sleeves could be used in the joint of the prefabricated part of wall to wall to confirm the connection strength. Modulization and industrialization is the main concerning of rapid reconstruction after earthquake hit area, and that also provides a large application perspective of this kind of composite shear wall.

Acknowledgements

The authors would like to thank for the financial support of NSFC (90815029, 51008226) and Kwang-Hua Fund for College of Civil Engineering in Tongji University.

References

Bozdogan, K.B. and Ozturk, D. (2008), "A method for static and dynamic analyses of stiffened multi-bay coupled shear walls", *Struct. Eng. Mech.,* **28**(4), 479-489.

Gong, Z.G., Lu, X.L. and Ji, S.Z. (2006), "Experimental study on seismic behavior of R.C. shear walls with different boundary restraints", *Struct. Eng.,* **22**(1), 56-61.

Holden, T., Restrepo, J. and Mander, J.B. (2003), "Seismic performance of precast reinforced and prestressed concrete walls", *J. Struct. Eng.,* **29**, 286-296.

Hossain, K.M.A. and Wright, H.D. (2004), "Design aspects of double skin composite framed shear walls in construction and service stages", *ACI Struct. J.*, **101**(1), 94-102.

Kabir, M.Z., Rezaifar, O. and Rahbar, M.R. (2007), "Upgrading flexural performance of prefabricated sandwich panels under vertical loading", *Struct. Eng. Mech.,* **26**(3), 227-295.

Lu, X.L. and Jiang, H.J. (2000), "Hysteretic analysis of a new type of energy dissipation shear walls" *Earthq. Eng. Eng. Vib.,* **20**(1), 112-119.

Mark, W. (2001), "Fabric-formed concrete structures", *Proceedings of the First International Conference on Concrete and Development C and D 1*, Tehran, April-May.

Ministry of Construction of the People's Republic of China (2002), *Code for Design of Concrete Structures,* GB50010-2002, China Architecture & Building Press. Beijing.

Ministry of Construction of the People's Republic of China (2008), *Code for Seismic Design of Building,* GB50011-2001, China Architecture & Building Press. Beijing.

People's Republic of China profession standard. JGJ3-2002 (2002), *Technical Specifications for High Rise Building Concrete Structure*, China Architecture & Building Press, Beijing. Saito, M., Yoshimatsu, T., Homma, K., *et al*. (1995), "Trusses and precast concrete slabs reinforced thereby", U.S. 5448866, Sep. 12.

Salonikios, T.N. and Kappos, A.J. (1999), "Cyclic load behavior of low slenderness reinforced concrete walls: Design basis and test results" *ACI Struct. J.*, **96**(48), 649-660.

Schmitz, R.P. (2006), "Fabric-formed concrete panel design", *Proceedings of the 17th Analysis and Computation Specialty Conference,* St. Louis, M0, United States, May.

Zhang, H.M., Lu, X.L., Lu, L. and Cao. W. (2007), "Influence of boundary element on seismic behavior of reinforced concrete shear walls", *J. Earthq. Eng. Eng. Vib.,* **27**(1), 92-99.